MOLECULAR AND CELLULAR BIOLOGY, Jan. 2009, p. 241–253 Vol. 29, No. 1
0270-7306/09/$08.00+0 doi:10.1128/MCB.01374-08

New Role for the Protein Tyrosine Phosphatase DEP-1 in Akt Activation and Endothelial Cell Survival[▽]

Catherine Chabot,[1] Kathleen Spring,[1] Jean-Philippe Gratton,[2,3,4] Mounib Elchebly,[5,6] and Isabelle Royal[1,3]*

CRCHUM-Centre Hospitalier de l'Université de Montréal and Institut du Cancer de Montréal, Montréal, Québec, Canada H2L 4M1[1]; Laboratory of Endothelial Cell Biology, Institut de Recherches Cliniques de Montréal, Montréal, Québec, Canada H2W 1R7[2]; Centre de Recherche de l'Hôpital Sainte-Justine, Montréal, Québec, Canada H3T 1C5[5]; and Departments of Medicine,[3] Pharmacology,[4] and Biochemistry,[6] Université de Montréal, Montréal, Québec, Canada

Received 29 August 2008/Accepted 6 October 2008

Functional inactivation of the protein tyrosine phosphatase DEP-1 leads to increased endothelial cell proliferation and failure of vessels to remodel and branch. DEP-1 has also been proposed to contribute to the contact inhibition of endothelial cell growth via dephosphorylation of vascular endothelial growth factor receptor 2 (VEGFR2), a mediator of vascular development. However, how DEP-1 regulates VEGF-dependent signaling and biological responses remains ill-defined. We show here that DEP-1 targets tyrosine residues in the VEGFR2 kinase activation loop. Consequently, depletion of DEP-1 results in the increased phosphorylation of all major VEGFR2 autophosphorylation sites, but surprisingly, not in the overall stimulation of VEGF-dependent signaling. The increased phosphorylation of Src on Y529 under these conditions results in impaired Src and Akt activation. This inhibition is similarly observed upon expression of catalytically inactive DEP-1, and coexpression of an active Src-Y529F mutant rescues Akt activation. Reduced Src activity correlates with decreased phosphorylation of Gab1, an adapter protein involved in VEGF-dependent Akt activation. Hypophosphorylated Gab1 is unable to fully associate with phosphatidylinositol 3-kinase, VEGFR2, and VE-cadherin complexes, leading to suboptimal Akt activation and increased cell death. Overall, our results reveal that despite its negative role on global VEGFR2 phosphorylation, DEP-1 is a positive regulator of VEGF-mediated Src and Akt activation and endothelial cell survival.

Angiogenesis, or the formation of new blood vessels from preexisting ones, is a tightly regulated process essential for development, female reproductive functions, and wound healing (16, 45). When uncontrolled or dysfunctional, angiogenesis also contributes to the development of several pathologies, including cancer, rheumatoid arthritis, retinopathies, and cardiovascular diseases (7, 32). In normal or pathological conditions, neovascularization relies on the ability of endothelial cells to respond to gradients of angiogenic factors, such as vascular endothelial growth factor (VEGF), which promotes the survival, permeability, migration, and proliferation of loosely associated endothelial cells as they form new capillary tubes (3, 14). At the surface of endothelial cells, the VEGF receptor 2 (VEGFR2) (KDR/Flk-1) receptor tyrosine kinase (RTK) has been identified as the major mediator of VEGF-dependent signaling and cellular activities (15). The tight coordination of phosphorylation and dephosphorylation events downstream of RTKs is required to maintain the proper signaling and kinetic specificities which dictate biological outcome. Control of tyrosine kinase-dependent signaling is in part mediated by protein tyrosine phosphatases (PTPs). However, despite the importance of VEGFR2 in the orchestration of the angiogenic response, the molecular mechanisms critical for the regulation of its signaling and biological activities are ill-defined, and little is known with respect to the implication of PTPs.

Density-enhanced phosphatase 1 (DEP-1, also known as PTP-η, CD148, or PTPRJ) is a receptor-type PTP of about 180 to 220 kDa which is expressed in several cell types, including endothelial, epithelial, and hematopoietic cells (6, 11, 26, 43). It comprises an extracellular domain containing eight fibronectin type III motifs, a transmembrane domain, and a single intracellular catalytic domain (43). The expression level of DEP-1 was initially reported to increase with cell density, suggesting that it might work as a regulator of cell contact-mediated growth inhibition (43). DEP-1 expression was also shown to be implicated in cell differentiation and the inhibition of tumor cell proliferation, suggesting a role as a tumor suppressor (31, 51, 54). In line with these findings, DEP-1 was identified as the gene associated with the mouse colon cancer susceptibility locus (*Scc1*) and is frequently found to be deleted or mutated in human cancers (47). In vivo inactivation of DEP-1 catalytic activity disrupts proper vascular development, leading to increased endothelial cell proliferation and impaired vessel remodeling and branching (50). Since VEGFR2 is a major promoter of vascular development, these observations suggested its potential interaction with DEP-1. Interestingly, a fraction of DEP-1 localizes at endothelial cell-cell junctions, where VEGFR2 has also been reported to associate (6, 8). Consistent with this colocalization, DEP-1 was shown to partly regulate VE-cadherin-mediated contact inhibition, via the concomitant dephosphorylation of VEGFR2 and inhibition of extracellular signal regulated kinase 1/2 (ERK1/2) activation (34). However, despite these important biological functions of

* Corresponding author. Mailing address: Centre de recherche du CHUM, Hôpital Notre-Dame, Pavillon J.A. de Sève Y-4605, 1560 rue Sherbrooke est, Montréal, Québec, Canada H2L 4M1. Phone: (514) 890-8000, ext. 25497. Fax: (514) 412-7591. E-mail: isabelle.royal@umontreal.ca.

▽ Published ahead of print on 20 October 2008.

DEP-1 in endothelial cells in vitro and in vivo, there is relatively little functional and mechanistic insight into how DEP-1 regulates the endothelial cell phenotype.

A few DEP-1 candidate substrates have been identified besides VEGFR2, including p120^{catenin}, Src, and the platelet-derived growth factor β (PDGF-β), Met/hepatocyte growth factor (HGF), epidermal growth factor (EGF), and RET receptors (4, 25, 30, 33, 36, 44). DEP-1 dephosphorylates specific tyrosine residues of PDGFR-β and Met/HGF receptors that are involved in the promotion of cell proliferation and morphogenesis, respectively (33, 44). In addition, DEP-1 overexpression in a malignant rat thyroid cell line was reported to specifically induce dephosphorylation of the Src-inhibitory Y529 and thus increase Src activity (36). Although DEP-1 was shown to negatively regulate the VEGF-dependent activation of ERK1/2 and DNA synthesis (34), the pattern of VEGFR2 dephosphorylation by DEP-1 as well as its potential implication in the regulation of other VEGF-dependent signaling cascades and biological activities remain unknown. In response to VEGF stimulation, VEGFR2 activates Src, phosphatidylinositol 3-kinase (PI3K), Akt, and endothelial NO synthase (eNOS), which provide cell survival, migratory, and permeability signals (1, 13, 18, 21, 22, 24, 40, 53). Activated VEGFR2 has been reported to associate with VE-cadherin complexes via β-catenin, and this is essential for its association with PI3K, the activation of Akt, and the promotion of cell survival in response to VEGF (8). In addition, we and others have recently shown that the Gab1 adapter protein recruits PI3K, associates with VEGFR2 complexes, and mediates optimal VEGF-dependent Akt activation, as well as endothelial cell migration and capillary formation (10, 35). In order to determine if a targeted action of DEP-1 was involved in the differential regulation of VEGF-evoked angiogenic pathways in endothelial cells, we investigated the consequences of DEP-1 expression on the VEGFR2 phosphorylation profile and downstream signaling. We show here that in contrast to other RTKs, DEP-1 expression induces the global dephosphorylation of VEGFR2 by targeting tyrosine residues in the kinase activation loop involved in VEGFR2 activation. Reciprocally, depletion of DEP-1 from endothelial cells results in the simultaneous increased phosphorylation of every major VEGFR2 autophosphorylation site. Unexpectedly, this does not translate into the upregulation of all VEGF-dependent signaling, since DEP-1 is required for dephosphorylation of Src-Y529 and consequent Src and Akt activation. Thus, the depletion of DEP-1 leads to the reduced Src-dependent phosphorylation of Gab1 and its decreased association with PI3K, Src, VE-cadherin, and VEGFR2 complexes, resulting in the inhibition of Akt activation and increased cell death. Our work therefore reveals an unforeseen role for DEP-1 in the association of Gab1 with the VEGFR2/VE-cadherin signaling complexes, the promotion of Src and Akt activation, and endothelial cell survival.

MATERIALS AND METHODS

Cell culture. HEK 293 cells were grown in high-glucose Dulbecco's modified Eagle's medium (DMEM; Invitrogen) containing 10% fetal bovine serum (FBS; Invitrogen) and 50 μg/ml gentamicin (Wisent). Human umbilical vein endothelial cells (HUVECs; Clonetics/Lonza or Cascade Biologics, purchased from Cedarlane Laboratories Ltd., Burlington, ON, Canada) were cultured (passages 1 to 4) on 0.2% gelatin-coated tissue culture dishes and maintained in endothelial basal medium 2 (EBM-2) supplemented with 2% FBS, EGF, VEGF, fibroblast growth factor (FGF), heparin, insulin-like growth factor 1, hydrocortisone, and ascorbic acid (EGM-2 bullet kit; Clonetics/Lonza).

Antibodies and reagents. Antibodies against phosphotyrosine (PY99), Myc (clone 9E10), VEGFR2 (clone C-1158 to immunoprecipitate VEGFR2 and clone A-3 for immunoblotting), Gab1 (clone H-198), and VE-cadherin (clone C-19 for immunoblotting) were purchased from Santa Cruz Biotechnology. A third anti-VEGFR2 antibody (rabbit antiserum) purchased from Upstate/Millipore (Cedarlane Laboratories) was also used to immunoprecipitate VEGFR2. Antibodies against VEGFR2 pY1054, VEGFR2 pY1059, the p85 subunit of PI3-kinase, phospholipase Cγ (PLCγ), glutathione *S*-transferase (GST), and Src (clone GD11 for immunoprecipitation) were obtained from Upstate/Millipore. Phospho-specific antibodies against VEGFR2 pY1054/1059, VEGFR2 pY1214, PLCγ pY783, Src pY529, and Src pY418 were obtained from BioSource Inc. (Invitrogen). Antibodies against VEGFR2 pY951, VEGFR2 pY996, VEGFR2 pY1175, Src (clone 36D10 for immunoblotting), Akt pS473, Akt pT308, Akt, ERK1/2 pT202/pY204, ERK1/2, eNOS pS1177, eNOS, FOXO1 pS256, FOXO1, p38 mitogen-activated protein kinase (MAPK) pT180/pY182, and p38 MAPK were from Cell Signaling Technology Inc., New England Biolabs. The VE-cadherin (clone 11D4.1 for immunoprecipitation) and β-catenin antibodies were from BD Transduction Laboratories, BD Biosciences. The actin (JLA20) monoclonal antibody developed by Jim Jung-Ching Lin was obtained from the Developmental Studies Hybridoma Bank developed under the auspices of the NICHD and maintained by The University of Iowa, Department of Biological Sciences, Iowa City. PP2 was purchased from Biomol (Plymouth Meeting, PA). Anti-VEGFR2 pY801 was generated as previously described (5). Horseradish peroxidase-conjugated anti-mouse or -rabbit immunoglobulin G antibodies from Cell Signaling Technology Inc. were used for immunodetection. VEGF, colony stimulating factor 1 (CSF-1), FGF, and the DEP-1 antibody were purchased from R&D Systems (distributed by Cedarlane Laboratories).

Generation of Myr–DEP-1 construct. The cDNA encoding the intracellular domain of human DEP-1 (amino acids 997 to 1337 [43]) was generated by reverse transcription-PCR carried out on total RNA extracted from HeLa cells with Trizol (Invitrogen) and using RNase H reverse transcriptase (Invitrogen) according to the manufacturer's instructions. Primers used were 5′-GTCGGATCCAGAAAGAAGAGGAAAGATGCA-3′ (sense orientation) and 5′-TTTCTCGAGGCGATGTAACCATTGGTCTT-3′ (antisense orientation). The underlined sequences correspond to added BamHI and XhoI restriction sites, respectively. The cDNA was cloned into the mammalian expression vector pCDNA4. The short myristylation sequence from the N-terminal domain of Src (amino acids 1 to 17) was introduced 5′ of the DEP-1 sequence to target the protein to the plasma membrane. The resulting Myr–DEP-1 cDNA expression vector encodes a fusion protein with an amino-terminal myristylation signal and amino acids 997 to 1337 of DEP-1 followed by a Myc tag and a His tag. DEP-1 point mutants (C1239S and D1205A) were generated by site-directed mutagenesis using the QuikChange site-directed mutagenesis kit according to the manufacturer's protocol (Stratagene, La Jolla, CA) and the following mutagenic primers (Invitrogen, Burlington, ON, Canada): 5′-CGATTCTGGTGCATTCCAGTGCTGGGGTCGG-3′ (C/S mutant, sense orientation) and 5′-CACCTCCTGGCCAGCCCACGGTGTTCCCGAC-3′ (D/A mutant, sense orientation). Mutations were confirmed by DNA sequencing.

Generation of the CSF-VEGFR2 chimeric receptor mutants. The CSF-VEGFR2 chimeric receptor encoding the human CSF-1 receptor extracellular domain fused to the transmembrane and intracellular domain of human VEGFR2 (in the pShuttle-CMV adenoviral vector; Qbiogene, MP Biomedicals, Montreal, QC, Canada) was generated as described before (35). The human CSF-1R (pSM-CSF-1R) and VEGFR2 (pCR3-hFlk1) vectors were kind gifts of Martine Roussel (St. Jude Children's Research Hospital, Memphis, TN) and Cam Patterson (University of North Carolina, Chapel Hill), respectively. All of the CSF-VEGFR2 mutations were generated using the QuikChange XL site-directed mutagenesis kit (Stratagene). The mutagenic primers (Invitrogen) used to generate the various mutants were the following: 5′-AACTGAAGACAGGCTTCTTGTCCATCGTCATGGATCC-3′ (Y801F), 5′-GTCAAGGGAAAGACTTCGTTGGAGCAATCCCTGTGGAT-3′ (Y951F), 5′-GAAGCTCCTGAAGATCTGTTTAAGGACTTCCTGACC-3′ (Y996F), 5′-CTGTGACTTTGGCTTGGCCCGGGATATTTTTAAAGATCCAG-3′ (Y1054F), 5′-GATATTTATAAAGATCCAGATTTTGTCAGAAAAGGAGATGCTCGC-3′ (Y1059F), 5′-TGCTCAGCAGGATGGCAAAGACTTCATTGTTCTTCCGA-3′(Y1175F), 5′-GACCCCAAATTCCATTTTGACAACACAGCAGGAATCAGTC-3′ (Y1214F). The Y1054F/Y1059F mutant was made on the CSF-VEGFR2 Y1059F mutant background by using the Y1054F mutagenic primer. The 5F mutant (Y801F/Y951F/Y996F/Y1175F/Y1214F) was sequentially made by using the corresponding mutagenic primers described above.

Substrate-trapping experiments. HEK 293 cells were seeded at 1.2×10^6 cells/10-cm dish and transfected 24 h later using the standard calcium phosphate method with 20 μg of VEGFR2 cDNA construct (pCR3-hFlk1), 15 μg of CSF-VEGFR2, or the corresponding pCR3 or pShuttle-CMV empty vectors. Twenty-four hours posttransfection, cells were serum starved in DMEM overnight. Prior to lysis, cells were incubated with freshly made pervanadate (100 μM) for 20 min at 37°C (the pervanadate mixture [10 mM] contained 1.0 ml of 10 mM sodium orthovanadate mixed with 1.2 μl of 30% H_2O_2). Cells were rinsed with phosphate-buffered saline (PBS) and lysed in a 50 mM HEPES, pH 7.5, buffer containing 0.5% Nonidet P-40, 0.5% Triton X-100, 10% glycerol, 150 mM NaCl, 1 mM EDTA, 1 mM phenylmethylsulfonyl fluoride, 10 μg/ml aprotinin, and 10 μg/ml leupeptin. The lysis buffer also contained 5 mM iodoacetic acid to inhibit cellular PTPs irreversibly. After incubation on ice for 20 min, dithiothreitol was added to a final concentration of 10 mM to inactivate unreacted iodoacetic acid. Cell lysates (4 mg and 2 mg of VEGFR2- and CSF-VEGFR2-transfected cells, respectively) were mixed with DEP-1 previously collected on beads. DEP-1 was immunoprecipitated for 1.5 h at 4°C using the 9E10 Myc antibody from independent lysates (250 μg, or 1 mg for the experiment shown below in Fig. 1A) of HEK 293 cells transfected with 10 μg of Myr–DEP-1 cDNA constructs per 10-cm dish. Protein G-Sepharose beads were added for 1.5 h at 4°C and then washed three times with lysis buffer (without iodoacetic acid) before incubation for three more hours with lysates of HEK 293 cells transfected with VEGFR2, CSF-VEGFR2, or empty vectors prepared as described above. Beads were washed three times with lysis buffer and trapped proteins were subjected to sodium dodecyl sulfate-polyacrylamide gel electrophoresis (SDS-PAGE), transferred onto Hybond-C Extra membranes (Amersham Biosciences/GE Healthcare), and revealed by Western blotting and enhanced chemiluminescence (ECL) detection according to the manufacturer's recommendations (Amersham Biosciences/GE Healthcare). HEK 293 cells expressing the CSF-VEGFR2 mutants were in addition stimulated at 37°C for 5 min with CSF-1 (50 ng/ml) at the end of the pervanadate treatment. For in vivo association, HEK 293 cells in 10-cm dishes were transfected with 10 μg of DEP-1 D/A plasmid (obtained from Nicholas Tonks, Cold Spring Harbor Laboratories) or with 10 μg of VEGFR2 plasmid (pCR3-hFlk1) in combination with 10 μg of pMT2 empty vector or 10 μg of DEP-1 D/A. Twenty-four hours posttransfection, cells were serum starved overnight, rinsed with PBS containing 1 mM Na_3VO_4, and lysed with the 50 mM HEPES, pH 7.5, lysis buffer described above (containing 5 mM NaF and 1 mM Na_3VO_4). VEGFR2 was immunoprecipitated overnight and further incubated for 1 h with protein A-Sepharose beads.

In vitro dephosphorylation of VEGFR2. HEK 293 cells were transfected with 20 μg of VEGFR2 cDNA construct (pCR3-hFlk1). Twenty-four hours posttransfection, cells were serum starved overnight, stimulated with VEGF (50 ng/ml) at 37°C for 5 min, and lysed as for the in vivo association experiment described above. VEGFR2 immunoprecipitates were washed twice with PBS and once with PTPase assay buffer (52) before incubating with 5 μg of GST or GST–DEP-1_{IC} fusion proteins (wild type [WT] or C/S) for 1 h at 37°C in 500 μl of PTPase buffer. GST–DEP-1_{IC} was generated by subcloning the intracellular domain of WT and C/S DEP-1 into pGEX4T2, and proteins were produced as described previously (46). VEGFR2 immunoprecipitates were washed three times with PTPase buffer before performing SDS-PAGE and Western blotting analysis.

Dephosphorylation of VEGFR2 by Myr–DEP-1 in HEK 293 cells. HEK 293 cells were transfected with 20 μg of VEGFR2 plasmid (pCR3-hFlk1) in combination with increasing amounts of WT Myr–DEP-1 plasmid (0, 0.05, 0.1, 0.2, 0.3, 0.4, 0.5, and 1.0 μg) per 10-cm dish. The total amount of DNA in each plate was normalized by using empty vector pCDNA4. Twenty-four hours posttransfection, the cells were serum starved overnight and stimulated or not with VEGF (50 ng/ml) for 2 min at 37°C. Cells were rinsed with 5 ml of PBS containing 250 μM Na_2VO_3 and lysed in the 50 mM HEPES, pH 7.5, lysis buffer containing 5 mM NaF and 250 μM Na_3VO_4. VEGFR2 was immunoprecipitated overnight at 4°C and further incubated for 1.5 to 2 h at 4°C with protein A-Sepharose beads. VEGFR2 immunoprecipitates were washed three times with lysis buffer and subjected to SDS-PAGE and Western blotting analysis.

Transfection and protein analysis in HUVECs. HUVECs (passage 3 or 4) were seeded at a density of 1×10^5 cells/cm^2 1 day before transfection. Pools of four specific DEP-1 (PTPRJ) small interfering RNAs (siRNAs; siGENOME SMARTpool catalog no. M-008476-01) and standard siCONTROL 2 or RISC-Free siRNAs (from Upstate/Dharmacon/Millipore) were transfected at a final concentration of 200 nM in high-glucose DMEM using Targefect reagents according to the manufacturer's recommendations (Targeting Systems Inc., Santee, CA). Similar results were obtained with either a RISC-free control siRNA pool or with the standard control 2 siRNA pool. The DEP-1 3 (Hs_PTPRJ_3_HP) and AllStars control siRNAs from Qiagen were also used for some of the experiments. After a 2-h incubation, cells were rinsed twice in PBS and cultured for 48 h in MCDB-131 medium (Sigma) supplemented with 2.0% FBS, 1 μg/ml hydrocortisone (Sigma), 10 ng/ml EGF, 15 μg/ml endothelial cell growth supplement (Upstate/Millipore), 50 μg/ml heparin sodium salt (Sigma), and 50 μg/ml gentamicin. HUVECs were next starved for 6 h in MCDB-131 medium containing 1% bovine serum albumin and 50 μg/ml gentamicin, with a medium change for the last hour. Cells were then incubated with VEGF (80 ng/ml) or other growth factors at 37°C for the indicated times, washed with PBS, and lysed on ice with the 50 mM HEPES, pH 7.5, lysis buffer containing 5 mM NaF and 2 mM Na_3VO_4. Immunoprecipitated proteins or total protein extracts (40 to 50 μg) were resolved by SDS-PAGE and transferred to nitrocellulose Hybond-C Extra membranes. Western blotting and ECL detection were then performed according to the manufacturer's recommendations. The Visualizer reagent (Upstate/Millipore) was sometimes used instead of ECL for detection of weak signals, such as that of DEP-1. For cDNA transfections, 5×10^4 cells/cm^2 were plated in 6-cm dishes and transfected the next day with Lipofectin according to the manufacturer's recommendations (Invitrogen). Five μg of empty vector (pMT2) or DEP-1 C/S plasmid, or combinations of 5 μg of DEP-1 C/S plasmid and 2 μg of either c-Src or c-Src^{Y529F} plasmids were transfected overnight in EBM. The transfection medium was then replaced with EGM-2 medium and the cells were stimulated 24 h later at 37°C with 50 ng/ml of VEGF after a 6-h starvation period in EBM. The full-length DEP-1 C/S human cDNA construct and pMT2 vector and the WT human Src and Src Y529F constructs (in pCDNA3) were generously provided by Nicholas Tonks (Cold Spring Harbor Laboratory) and Stéphane Laporte (McGill University), respectively.

In vitro Src kinase assay. Src immunoprecipitates were washed three times with the 50 mM HEPES, pH 7.5, lysis buffer containing 5 mM NaF and 1 mM Na_3VO_4 and once with PBS before adding the Src peptide substrate with [γ-^{32}P]ATP in a Src kinase reaction buffer (Src kinase assay kit; catalog no. 17-131; Upstate/Millipore). After a 10-min incubation at 30°C, the phosphorylated peptide was precipitated with 40% trichloroacetic acid, separated from the residual [γ-^{32}P]ATP using P81 phosphocellulose paper, and quantified with a scintillation counter.

Cell death evaluation. HUVECs were transfected with siRNAs as described above. Following treatment, cells were trypsinized and plated at a density of 3×10^4/cm^2 in complemented MCDB131 medium and allowed to adhere for 18 h. The cells were then washed with PBS and incubated for 33 h in EBM containing 2% FBS alone, with VEGF (80 ng/ml), or VEGF (80 ng/ml) with FGF (80 ng/ml) and heparin (5 μg/ml). At the end of this incubation period, floating and trypsin-detached HUVECs were collected and washed once with cold PBS and fixed in 70% cold ethanol (overnight at −20°C). After fixation, cells were stained for 30 min in PBS with RNase A (200 μg/ml) and propidium iodide (50 μg/ml). DNA content was analyzed by fluorescence-activated cell sorting. At least 10,000 events were analyzed. Dead cells were defined as sub-2*N* DNA-containing cells (sub-G_1 peak).

RESULTS

DEP-1 targets Y1054/Y1059 in the VEGFR2 kinase activation loop. Depletion of DEP-1 in VEGF-stimulated confluent endothelial cells results in increased VEGFR2 phosphorylation, suggesting that VEGFR2 is a substrate of DEP-1 (34). However, the specific VEGFR2 tyrosine residues targeted for dephosphorylation as well as the general consequences on VEGF-induced signaling remain ill-defined. To first confirm that VEGFR2 is a bona fide DEP-1 substrate, we initially investigated the ability of the substrate-trapping mutant DEP-1 D1205A (D/A) to interact with VEGFR2. For this purpose, the myristylated and Myc-tagged intracellular portion of DEP-1 D/A (Myr-DEP-1 D/A) was immunoprecipitated from transfected HEK 293 cells and immobilized on protein G-coupled Sepharose beads. The intracellular portions of WT DEP-1 and C1239S (C/S) catalytically inactive mutant were also purified. Lysates of pervanadate-treated HEK 293 cells transfected with vector alone (pCR3) or expressing either full-length VEGFR2 or a CSF-VEGFR2 chimera, which encompasses the CSF-1 receptor extracellular domain fused to the transmembrane and intracellular domains of VEGFR2, were then incubated with Myr-DEP-1 D/A-, WT- and C/S-coupled

beads. As shown in Fig. 1A, VEGFR2 or the CSF-VEGFR2 chimera formed stable complexes with the D/A mutant, but as expected, VEGFR2 did not stably associate with the WT Myr–DEP-1. Under identical conditions, the catalytically inactive C/S mutant was unable to trap VEGFR2 or other tyrosine-phosphorylated proteins. The association of CSF-VEGFR2 with Myr-DEP-1 D/A was blocked by sodium vanadate, a competitive inhibitor of PTPs which interacts with the catalytic site and blocks recognition of substrates, suggesting that VEGFR2 can associate with the active site of DEP-1 (Fig. 1B) (28). VEGFR2 could also coimmunoprecipitate with full-length DEP-1 D/A in transfected HEK 293 cells (Fig. 1C). This association led to the increased phosphorylation of VEGFR2 when compared to VEGFR2 expressed alone, demonstrating that VEGFR2 was protected from dephosphorylation by this interaction with the D/A substrate-trapping mutant. Lastly, in agreement with VEGFR2 being a DEP-1 substrate, incubation of immunoprecipitated VEGFR2 with the intracellular portion of DEP-1 fused to GST (GST–DEP-1_{IC}) led to its dephosphorylation, while its phosphorylation was maintained when incubated with the catalytically inactive C/S mutant (Fig. 1D). Thus, altogether, these results demonstrate the functional interaction between VEGFR2 and DEP-1 and, together with previous siRNA studies, further validate VEGFR2 as a DEP-1 substrate (34).

The PDGF-β and Met/HGF receptors have been identified as DEP-1 substrates (33, 44). In these particular cases, DEP-1 dephosphorylates specific tyrosine residues previously recognized as mediators of proliferation and morphogenesis, respectively. To define the impact of DEP-1 on VEGFR2 function, we initially investigated if DEP-1 had specificity toward any major VEGFR2 autophosphorylation sites. For this, HEK 293 cells were cotransfected with VEGFR2 (20 μg) and increasing amounts of WT Myr–DEP-1 (0, 0.05, 0.1, 0.2, 0.3, 0.4, 0.5, and 1 μg), similarly to what had been done for Met (44). Figure 2 shows that in contrast to the PDGF-β and Met/HGF receptors, VEGFR2 tyrosine phosphorylation was globally attenuated by DEP-1. Thus, a gradual and simultaneous decrease in the level of phosphorylation of all major autophosphorylation sites tested was observed as the expression of Myr–DEP-1 increased, including that of Y996 in the kinase insert domain (Y951 was not phosphorylated in HEK 293 cells), Y1054/Y1059 in the kinase activation loop, and Y1175 and Y1214 in the C-terminal tail. Quantification of the results from five independent experiments confirmed this interpretation (Fig. 2B). These findings further reveal that as the phosphorylation level of Y1054/Y1059 progressively decreases, the phosphorylation of Y996, Y1214, and Y1175 decreases proportionally while maintaining the same differential phosphorylation ratios that are also similarly observed in unstimulated quiescent cells. These results therefore suggest that the autoactivation residues Y1054 and Y1059 are targeted by DEP-1 and that this results in the inhibition of kinase activity and the consequent general dephosphorylation of VEGFR2.

To validate this hypothesis, we next evaluated the ability of Myr–DEP-1 D/A to trap various CSF-VEGFR2 mutants encompassing either single Y/F mutations of every major autophosphorylation sites, the double Y1054F/Y1059F mutation, or five Y/F mutations corresponding to all major autophosphorylation sites except Y1054 and Y1059 (5F mutant; Y801F, Y951F, Y996F, Y1175F, and Y1214F) (Fig. 3). Lysates of pervanadate-treated and CSF-1-stimulated HEK 293 cells transfected with vector alone (pShuttle) or expressing CSF-VEGFR2 WT and mutants were incubated with Myr–DEP-1 D/A previously immobilized on beads. Lysates of cells expressing WT CSF-VEGFR2 were also incubated with beads coupled or not to WT DEP-1 as negative controls. Results showed that Myr–DEP-1 D/A retained the ability to trap all single Y/F mutants; slight variations in recovery observed between some of the single mutants were not considered significant. However, Myr–DEP-1 D/A clearly failed to efficiently trap the Y1054/1059F double mutant, suggesting that the autoactivation loop tyrosines were recognized by the DEP-1 catalytic site (Fig. 3A). Conversely, Myr–DEP-1 D/A could still trap the 5F mutant, which retains Y1054 and Y1059 but not any of the other major autophosphorylation sites (Fig. 3B). Importantly, the phosphorylation levels of all mutants were similar in these experiments, confirming that the decreased association of the VEGFR2 Y1054F/Y1059F mutant with Myr–DEP-1 D/A was due to the loss of these tyrosine residues and not because it was less phosphorylated overall compared to other mutants (Fig. 3C). Collectively, these data thus support a model where the VEGFR2 autoactivation residues are targeted by DEP-1, resulting in the simultaneous dephosphorylation of all autophosphorylation sites.

Silencing of DEP-1 in confluent endothelial cells leads to the increased phosphorylation of all major VEGFR2 autophosphorylation sites but differentially affects VEGF-induced signaling pathways. If DEP-1 is involved in the global dephosphorylation of VEGFR2, the depletion of DEP-1 should then lead to the overall increase of VEGFR2 phosphorylation and activation of downstream signaling cascades. To test this hypothesis, the phosphorylation of VEGFR2 was investigated in DEP-1-depleted endothelial cells. Confluent HUVECs were transfected with control or DEP-1 siRNA pools and the VEGF-induced phosphorylation of all major autophosphorylation sites evaluated at the indicated times using phospho-specific antibodies (Fig. 4). As postulated, the phosphorylation of every tyrosine residue tested (Y801, Y951, Y996, Y1054, Y1059, Y1175, and Y1214) was similarly increased in DEP-1-depleted cells, as early as 2 min and up to 15 min poststimulation. Our results thus show that DEP-1 regulates global VEGFR2 phosphorylation, suggesting that DEP-1 could regulate a broad range of VEGFR2-dependent signaling pathways. To investigate this, lysates of HUVECs treated as above were probed with phospho-specific antibodies recognizing the active forms of major enzymes known to be stimulated in response to VEGF. Consistently, with kinetics similar to those observed for the increased phosphorylation of VEGFR2, the phosphorylation of PLCγ, eNOS, ERK1/2, and p38 was upregulated in DEP-1-depleted cells compared to control cells (Fig. 5A). Surprisingly, however, the phosphorylation of Akt (on S473 and T308) was consistently impaired in DEP-1-depleted cells (Fig. 5A and B). Moreover, the phosphorylation of the Akt substrates FOXO1/4, which are involved in the regulation of cell survival, was also reduced by the depletion of DEP-1 (Fig. 5B). Thus, although VEGFR2 autophosphorylation sites known to be involved in the activation of all of these pathways were upregulated in DEP-1-depleted cells (5, 41),

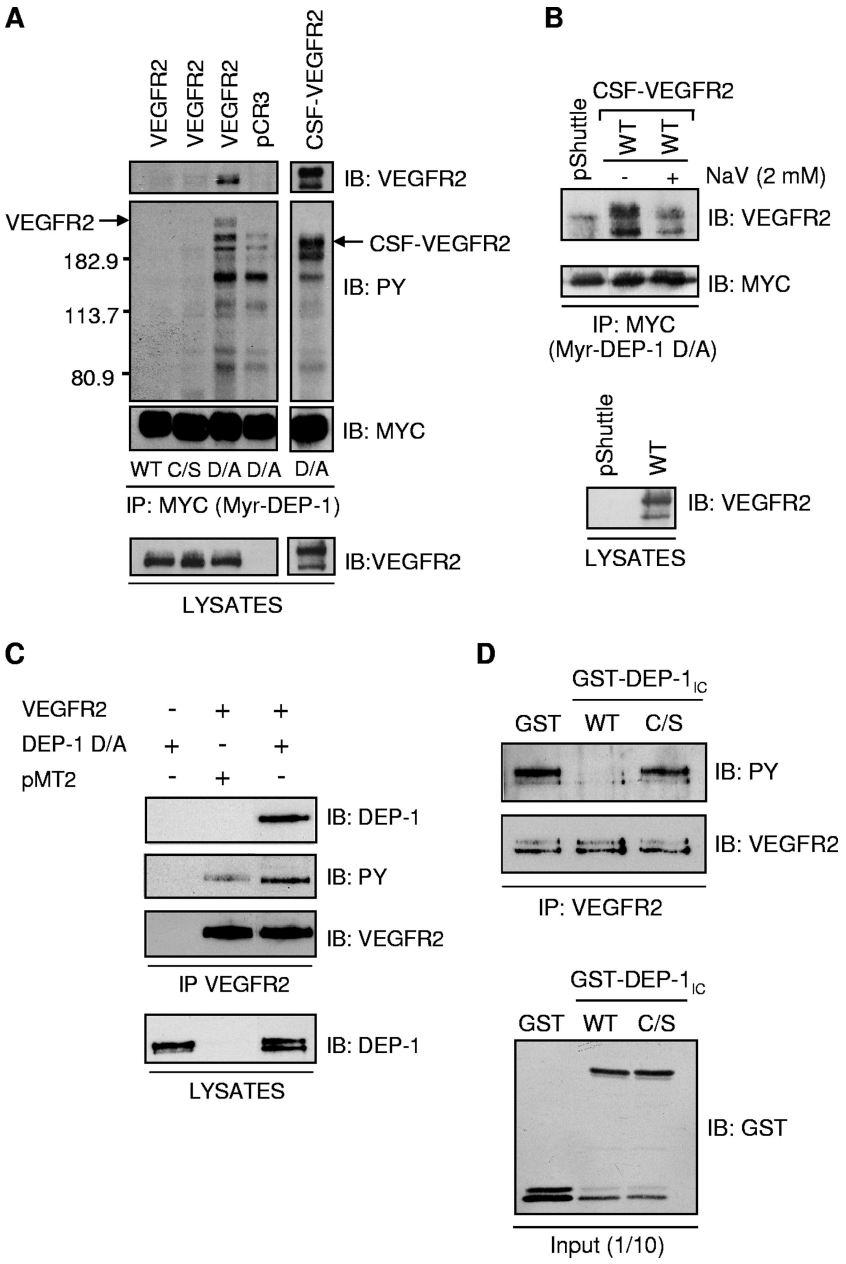

FIG. 1. VEGFR2 and the CSF-VEGFR2 chimera are substrates of DEP-1. (A) Lysates of pervanadate-treated HEK 293 cells transfected with vector alone (pCR3), VEGFR2, or the CSF-VEGFR2 chimera were incubated with the Myc-tagged, myristylated intracellular domain of WT DEP-1 (Myr-DEP-1) or the C/S and D/A mutants previously immobilized on protein G-coupled Sepharose beads by using the Myc antibody (clone 9E10). Interacting receptors were detected using the VEGFR2 monoclonal antibody (A-3). Immunoblotting (IB) with the Myc antibody revealed similar levels of immunoprecipitated (IP) DEP-1. The upper membrane was stripped and reprobed with the phosphotyrosine monoclonal antibody PY99 (PY) to visualize the complete spectrum of tyrosine-phosphorylated proteins that interacted with DEP- D/A but not with the WT or C/S mutant. Immunodetection of VEGFR2 and CSF-VEGFR2 in lysates (40 μg) of pervanadate-treated transfected HEK 293 cells confirmed their similar levels of expression under all conditions. (B) Addition of the PTP competitive inhibitor sodium vanadate (NaV; 2 mM) to the substrate-trapping reaction mixture blocks the interaction of CSF-VEGFR2 with the Myr-DEP-1 D/A mutant. pShuttle, empty vector. (C) VEGFR2 was immunoprecipitated from lysates of HEK 293 cells transfected with full-length DEP-1 D/A alone or with VEGFR2 cotransfected with either vector alone (pMT2) or DEP-1 D/A. The coprecipitation of DEP-1 D/A with VEGFR2 was detected by Western blotting using the DEP-1 antibody, while the tyrosine phosphorylation of VEGFR2 was revealed using the phosphotyrosine antibody PY99 (PY). Immunodetection of immunoprecipitated VEGFR2 and of DEP-1 D/A in total cell lysates confirmed their similar levels of expression. (D) VEGFR2 was immunoprecipitated from transfected HEK 293 cells stimulated with VEGF (50 ng/ml) for 5 min. Immunoprecipitates were incubated with GST or GST–DEP-1_{IC} fusion proteins encompassing the intracellular domain of WT DEP-1 or the C/S mutant. The VEGFR2 tyrosine phosphorylation level was detected using the phosphotyrosine antibody PY99 (PY). Immunoblotting with VEGFR2 and GST antibodies showed equal levels of immunoprecipitated VEGFR2 and GST fusion proteins that were added to the dephosphorylation reaction mixture.

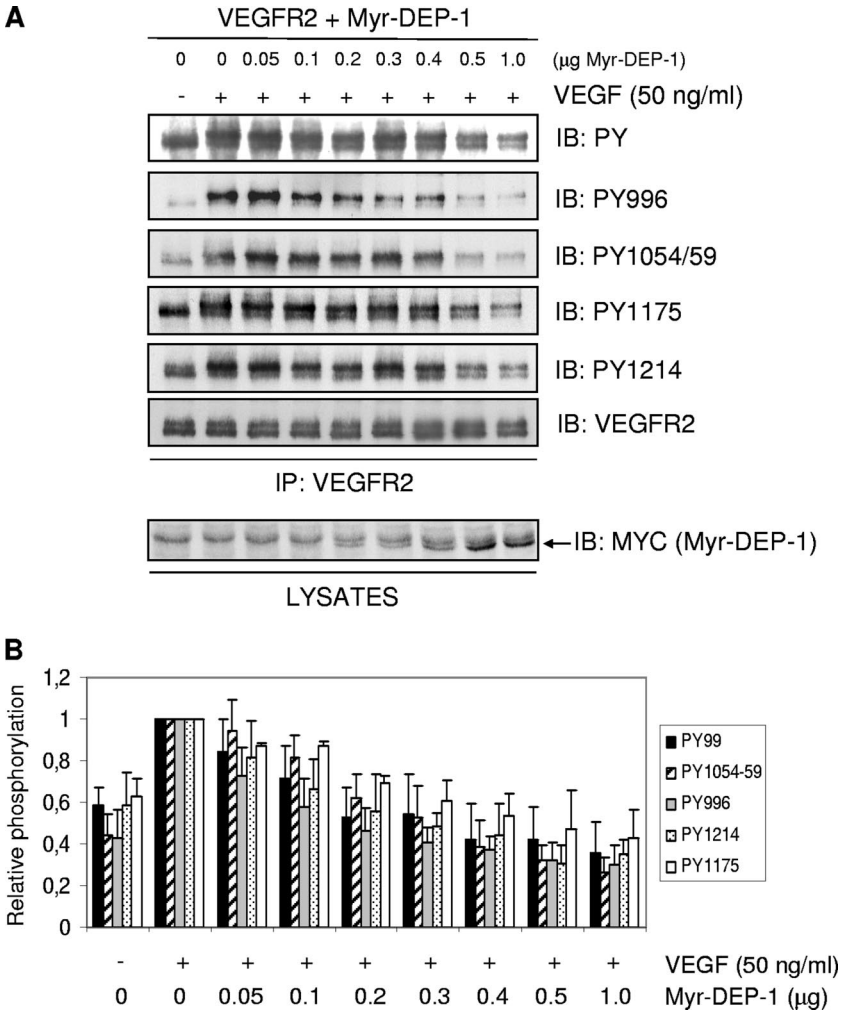

FIG. 2. DEP-1 leads to the global dephosphorylation of VEGFR2. (A) HEK 293 cells were transfected with 20 μg of VEGFR2 cDNA and increasing amounts of WT Myr-DEP-1 cDNA. Cells were serum starved, stimulated with VEGF (50 ng/ml) for 2 min, and lysed. VEGFR2 was immunoprecipitated (IP) (C-1158 antibody), and its global phosphorylation was revealed using the phosphotyrosine antibody PY99 (PY). The phosphorylation levels of Y996, Y1054/1059, Y1175, and Y1214 were detected by immunoblotting (IB) with phospho-specific VEGFR2 antibodies. Membranes were stripped and immunoblotted with the VEGFR2 antibody (A-3) to show a constant level of immunoprecipitated VEGFR2 (one representative blot shown). Lysates of transfected HEK 293 cells (40 μg) were immunoblotted with the Myc antibody (9E10 clone) to detect increasing Myr-DEP-1 expression levels. (B) Results obtained from five independent experiments were quantified using the Bio-Rad Quantity One analysis software. The relative phosphorylation intensity of each VEGFR2 phosphotyrosine residue was determined and normalized according to the amount of VEGFR2 immunoprecipitated under each condition.

this did not translate into the enhancement of VEGF-dependent Akt activation.

DEP-1 mediates VEGF-dependent Akt activation through the Src-dependent tyrosine phosphorylation of Gab1 and associated PI3K. The phosphorylation of the scaffolding adapter Gab1 by Src kinases and its association with PI3K has been reported to mediate Akt activation in VEGF-stimulated microvascular endothelial cells and HUVECs (10, 35). Since DEP-1 is able to dephosphorylate the inhibitory Y529 and activate Src (36), we hypothesized that the inhibition of Akt in the absence of DEP-1 could be a direct consequence of reduced Src activation and Gab1 phosphorylation. As initial support for this hypothesis, we found that incubation of HUVECs with the Src family kinase inhibitor PP2 led to the complete block of Akt phosphorylation on S473 in response to VEGF stimulation, demonstrating that in VEGF-stimulated HUVECs, Akt activation is Src kinase dependent (Fig. 6A). To then determine if Src activity was regulated by DEP-1, total cellular Src was immunoprecipitated from control and DEP-1-depleted cells stimulated or not with VEGF. Immunoblot analysis using the p^{Y418}Src antibody revealed that Src was less phosphorylated in DEP-1-depleted cells (Fig. 6B). Consistently, the ability of immunoprecipitated Src to phosphorylate a Src-specific peptide substrate was decreased in VEGF-stimulated DEP-1-depleted cells, demonstrating that the reduced phosphorylation of Y418 correlated with a strong inhibition of Src kinase activity (1.3-fold induction over unstimulated control cells compared to a 3.6-fold induction in VEGF-stimulated control cells) (Fig. 6C). However, we were not able to see modulations of the phosphorylation of Y529 on total Src between control and DEP-1-depleted cells. Since DEP-1 localizes at cell-cell junctions in endothelial

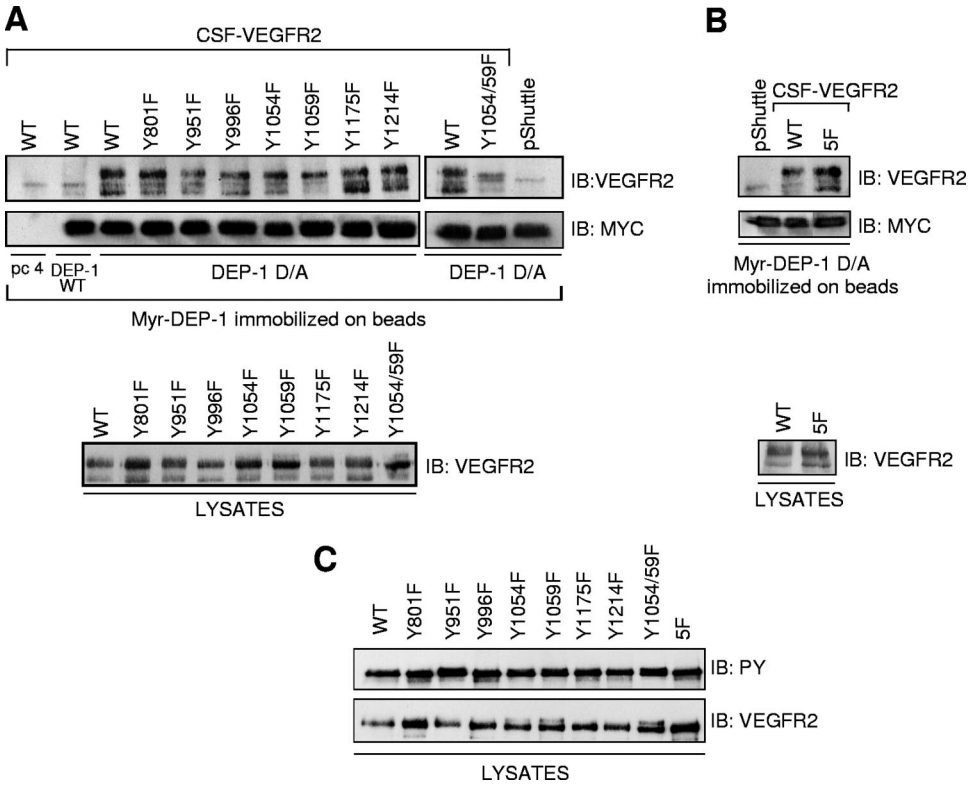

FIG. 3. DEP-1 D/A traps VEGFR2 via tyrosine residues in the activation loop. (A) HEK 293 cells were transfected with empty vector (pShuttle) or cDNA constructs encoding the WT CSF-VEGFR2, single Y/F mutants of every major VEGFR2 autophosphorylation site, and the double Y1054/1059F mutant. Following treatment of the cells with pervanadate and stimulation with CSF-1 (50 ng/ml) for 5 min, cells were lysed and incubated with Myr-DEP-1 D/A immobilized on protein G-coupled Sepharose beads as described in Materials and Methods. As negative controls, cell lysates expressing WT CSF-VEGFR2 were also incubated with beads alone (pc4, pCDNA4-transfected cells) or with WT Myr-DEP-1-coupled beads. The trapped receptors were immunodetected with VEGFR2 (A3) antibody on the upper part of the membrane while equal amounts of immunoprecipitated (IP) Myr-DEP-1 were detected with the Myc (9E10 clone) antibody. The lower panel shows similar amounts of WT and mutant CSF-VEGFR2 expressed in HEK 293 cell lysates (40 μg). (B) The same substrate-trapping experiment was performed using the CSF-VEGFR2 5F mutant harboring the Y801F, Y951F, Y996F, Y1175F, and Y1214F mutations. (C) The phosphorylation status of the CSF-VEGFR2 mutants under the experimental conditions used for the trapping experiments was determined. Note the similar levels of tyrosine phosphorylation of the various mutants.

cells and the VE-cadherin-associated pool of Src represents an important fraction of activated Src in response to VEGF (23, 25, 44, 49), we investigated the phosphorylation of Y529 of VE-cadherin-associated Src. Figure 6D shows that the depletion of DEP-1 greatly enhanced Y529 phosphorylation of this pool of Src, consistent with the observed reduction of Src kinase activity in VEGF-stimulated DEP-1-depleted cells. These data demonstrate that DEP-1 contributes to the activation of Src in endothelial cells, presumably by dephosphorylating the Y529-inhibitory residue of Src associated with VE-cadherin complexes. Moreover, these results also strongly suggest that reduced Src activity, resulting from the depletion of DEP-1, is responsible for the decreased Akt activation in response to VEGF stimulation. To further prove the role of DEP-1 and Src in VEGF-mediated Akt activation, the DEP-1 C/S catalytically inactive mutant was expressed in HUVECs. Results from Fig. 6E show that Src and Akt were concomitantly inhibited upon VEGF-stimulation of these cells, compared to their activation in control cells transfected with empty vector (pMT2). Importantly, coexpression of the constitutively active Src Y529F mutant with DEP-1 C/S was able to rescue Akt activation upon VEGF stimulation (Fig. 6F). These data therefore convincingly demonstrate that DEP-1 is required for full Src activation in VEGF-stimulated cells and that this is essential for the optimal activation of Akt.

Based on this, we next investigated if the Src-dependent phosphorylation of Gab1 was also defective in DEP-1-depleted cells, thus explaining Akt inhibition. The level of Gab1 tyrosine phosphorylation and its ability to associate with signaling proteins were therefore evaluated in VEGF-stimulated DEP-1-depleted cells (Fig. 7). Significantly, the tyrosine phosphorylation of immunoprecipitated Gab1 was inhibited in DEP-1-depleted cells (Fig. 7A). The ability of Gab1 to associate with Src in response to VEGF was also reduced, suggesting that in addition to the inhibition of Src activity in VEGF-stimulated DEP-1-depleted cells, this impaired ability of Src to associate with Gab1 may also contribute to the decreased Gab1 tyrosine phosphorylation (Fig. 7A). Importantly, the ability of hypophosphorylated Gab1 to associate with the p85 subunit of PI3K was greatly reduced in these cells (Fig. 7B). Overall, these experiments show that the depletion of DEP-1 results in the suboptimal Src activation in response to VEGF stimulation, the ensuing reduced Gab1 phosphorylation and association with Src and PI3K, and the consequent down-regulation of Akt activation.

Carmeliet et al. reported that the formation of a complex

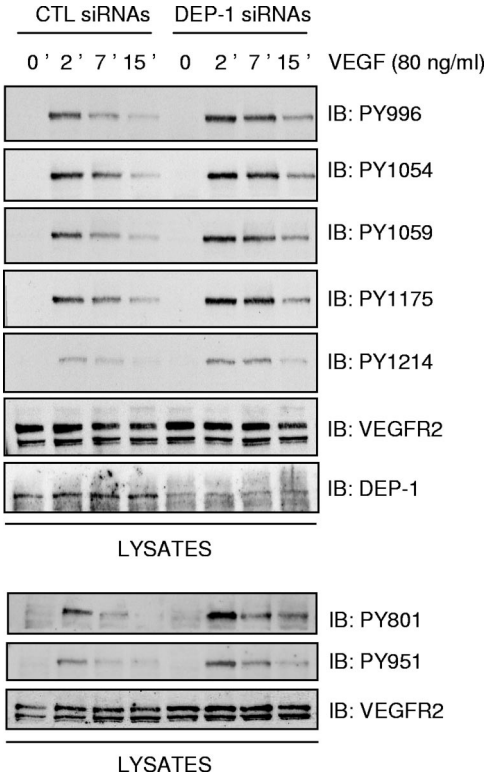

FIG. 4. Depletion of DEP-1 leads to the global increase in tyrosine phosphorylation of VEGFR2. HUVECs transfected with control (CTL) or DEP-1 siRNAs were incubated in full medium for 48 h, after which time cells were starved for 6 h and then stimulated with VEGF (80 ng/ml) for the indicated times. Cell lysates (50 μg) were immunoblotted (IB) on different membranes with VEGFR2 (clone A3) or phospho-specific VEGFR2 antibodies. The depletion of DEP-1 was confirmed by immunoblotting the cell lysates with the DEP-1 antibody. The last three panels are from an independent experiment.

between VEGFR2, VE-cadherin, β-catenin, and PI3K is required for Akt activation and the survival of endothelial cells (8). Since Gab1 associates with PI3K and VEGFR2 and mediates VEGF-induced Akt activation (35), we investigated if Gab1 was also part of this complex in HUVECs. Figure 8 shows that immunoprecipitated Gab1 associates with PI3K, β-catenin, VE-cadherin, and VEGFR2, strongly suggesting that Gab1 mediates the association of PI3K to the VEGFR2/VE-cadherin complex in response to VEGF stimulation. However, the association of Gab1 with all of these proteins was impaired by the depletion of DEP-1. Collectively, these experiments reveal an essential and unsuspected role for DEP-1 as a mediator of VEGF-induced Gab1 tyrosine phosphorylation and downstream Akt activation in endothelial cells. In addition, our observations also underscore the ability of Gab1 to associate with the VEGFR2/VE-cadherin complex and show that this event is positively regulated by DEP-1.

Depletion of DEP-1 impairs endothelial cell survival promoted by VEGF. Akt is essential for VEGF-mediated cell survival (8, 18, 21). The decrease of Akt activation observed in VEGF-stimulated DEP-1-depleted cells suggests that VEGF will not be as efficient in protecting these cells from cell death under starvation conditions. To test this, control and DEP-1-depleted HUVECs seeded on gelatin-coated plates were incubated in EBM supplemented with 2% FBS only, in the absence or presence of VEGF, for 33 h. At the end of this incubation, cells were collected and stained with propidium iodide, and the DNA content was analyzed by fluorescence-activated cell sorting (FACS). Cell death was quantified by the percentage of hypodiploid cells (sub-G_1 population). The basal level of cell death in starved control and DEP-1-depleted cell populations was normalized to assess the relative efficacy of VEGF in the promotion of their survival. In the control cell population, the presence of VEGF decreased cell death by an average of 43%. In contrast, VEGF showed no protective effects on DEP-1-depleted cell populations (Fig. 9A). The combination of VEGF with FGF, another endothelial cell survival factor, led to an even greater reduction of control cell death (an average of 79%). In the case of DEP-1-depleted cells, the addition of FGF also led to a significant but smaller reduction of cell death (an average of 37%). Consistent with these data, Src and Akt activation were impaired in DEP-1-depleted cells in response to FGF stimulation (Fig. 9B). Altogether, these results indicate for the first time that DEP-1 is involved in the promotion of VEGF- and growth factor-mediated cell survival via activation of the Akt pathway.

DISCUSSION

The in vivo functional inactivation of DEP-1 following the substitution of its intracellular catalytic domain with green fluorescent protein leads to impaired vascularization characterized by increased proliferation of endothelial cells and defective remodeling and branching (50). Since VEGFR2-dependent pathways are essential for proper vascular development, these studies suggested that part of the observed phenotype was due to their defective regulation in the absence of functional DEP-1. An elegant study by Lampugnani et al. supported this interpretation and further proposed that DEP-1, which colocalizes with cell-cell junctions, was involved in the VE-cadherin-mediated cell contact inhibition, via the dephosphorylation of VEGFR2 and inhibition of the proliferative ERK1/2 pathway in confluent endothelial cells (34). However, despite the connection made, no direct interaction between VEGFR2 and DEP-1 was described, and the broad consequences of DEP-1 expression on VEGF-stimulated endothelial cells remained undefined. In this paper, we show that VEGFR2 and DEP-1 physically associate via the catalytic site of DEP-1. Our findings support the view that VEGFR2 tyrosine residues in the activation loop are targeted by DEP-1 and that this results in reduced kinase activation and the consequent general decrease of VEGFR2 autophosphorylation. Conversely, the depletion of DEP-1 leads to the overall increased phosphorylation of VEGFR2, as early as 2 min post-VEGF stimulation, but unexpectedly, not to the overall stimulation of VEGF-dependent signaling. Our major finding is that DEP-1 is a positive regulator of VEGF-induced Src and Akt activation, as well as of endothelial cell survival. We show that this is most likely due to the essential function of DEP-1 in allowing the Src kinase-dependent phosphorylation of the Gab1 adapter, which was previously shown to mediate Akt activation in VEGF-stimulated endothelial cells through its ability to associate with PI3K (Fig. 10) (10, 35). Consistently, in DEP-1-depleted cells, hypophosphorylated Gab1 no longer associates with PI3K, Src, and other components of the

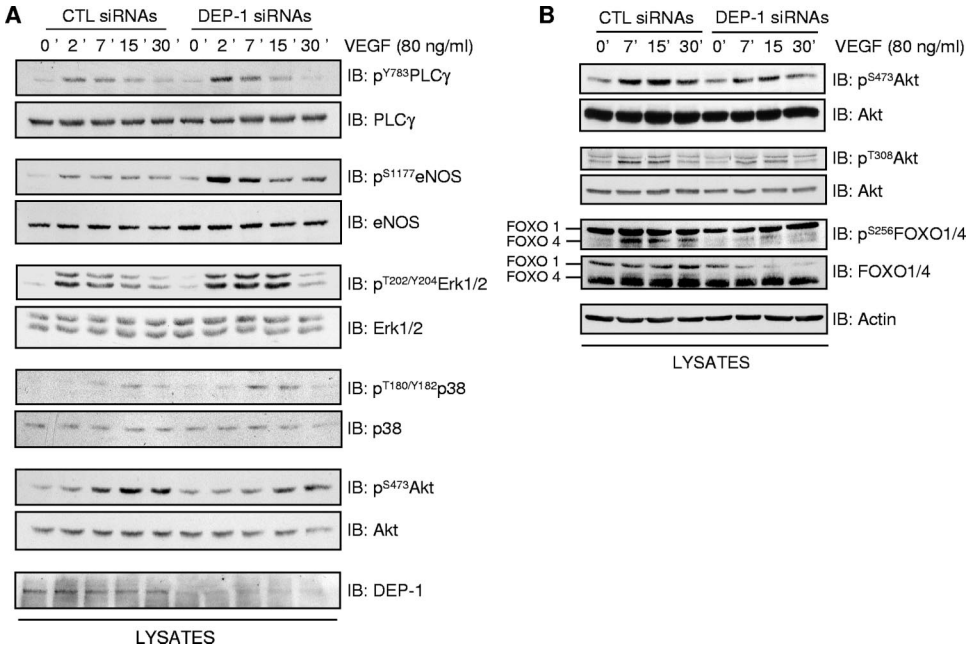

FIG. 5. Depletion of DEP-1 does not lead to the general enhancement of VEGF-dependent signaling. (A and B) Confluent HUVECs were transfected and treated as for Fig. 4. Phosphorylation of PLCγ, eNOS, ERK1/2, p38, Akt (S473 and T308 phosphorylation), and FOXO1/4 was evaluated by immunoblotting (IB) cell lysates (40 μg) with phospho-specific antibodies. The membrane sections were stripped and blotted with the corresponding antibodies to show equal protein loading. The depletion of DEP-1 was confirmed by immunoblotting the cell lysates with the DEP-1 antibody. Blots shown in panels A and B are from independent experiments.

VE-cadherin complex. Our work thus importantly reveals that through DEP-1-mediated Src activation, phosphorylated Gab1 recruits PI3K to the VE-cadherin, β-catenin, and VEGFR2 complex previously shown to allow Akt activation and endothelial cell survival (8).

Previous work by Lampugnani and colleagues suggested that VE-cadherin-dependent inhibition of cell growth was mediated via the dephosphorylation of VEGFR2 by DEP-1 at cell-cell junctions, where both have been reported to localize (6, 8, 34). Since VE-cadherin function has also been associated with the ability of VEGF to promote endothelial cell survival (8), this led to the idea that as cells reached confluence, DEP-1 might specifically dephosphorylate VEGFR2 autophosphorylation sites involved in ERK1/2 activation and proliferation, but not those involved in Akt activation and survival. Thus, in a manner analogous to the targeted dephosphorylation of the PDGF-β and Met/HGF receptors by DEP-1 (33, 44), specific dephosphorylation of VEGFR2 would explain the opposite regulation of VE-cadherin on cell proliferation and survival. What our study has shown is that there is indeed a differential regulation of ERK1/2 and Akt activation by DEP-1 in endothelial cells. DEP-1 downregulates VEGF-mediated ERK1/2 activation, as well as that of PLCγ, p38, and eNOS, but surprisingly, positively regulates Akt activation. However, this is not dictated by a differential dephosphorylation of VEGFR2 by DEP-1. Our experiments involving DEP-1 overexpression, the trapping of VEGFR2 Y/F mutants, or the impact of DEP-1 siRNAs on VEGFR2 phosphorylation collectively suggest that DEP-1 induces global VEGFR2 dephosphorylation via the preferential dephosphorylation of Y1054 and Y1059 in the activation loop. In fact, an in-depth analysis of VEGF-dependent signaling in DEP-1-depleted cells rather reveals that inhibition of Src, which has also been identified as a DEP-1 substrate (36), is more likely responsible for the inhibition of Akt. First, we found that the direct inhibition of Src kinases by PP2 was sufficient to block Akt activation in response to VEGF. In addition, the phosphorylation of Src on Y418 and its dephosphorylation on inhibitory Y529 were both found to be impaired in DEP-1-depleted cells, consistent with the observed inhibition of its kinase activity at times when Akt activation was also reduced. Lastly, expression of the catalytically inactive DEP-1 C/S mutant in VEGF-stimulated HUVECs was also shown to lead to the concomitant inhibition of Src and Akt phosphorylation on Y418 and S473, respectively, and coexpression of the constitutively active Src mutant (Y529F) was shown to rescue Akt phosphorylation. These results are therefore consistent with the reported ability of DEP-1 to activate Src kinases via dephosphorylation of the inhibitory C-terminal Y529 (36, 55), and hence, strongly support Src as a DEP-1 substrate in endothelial cells. We further showed that the phosphorylation of the Gab1 adapter, which is PP2 sensitive and required for the optimal VEGF-dependent activation of Akt (10, 35), was also blocked in DEP-1-depleted cells. Altogether, these data thus reveal a new role for DEP-1 as an important mediator of VEGF-induced activation of Src, Gab1, PI3K, Akt, and consequently, of endothelial cell survival. Given that Src is upstream of Akt activation in many cell systems, DEP-1 could represent a major mediator of cell survival in various cellular contexts. Consistent with this idea, we have shown that DEP-1 is also required for the optimal FGF-mediated activation of Src, Akt, and endothelial cell survival.

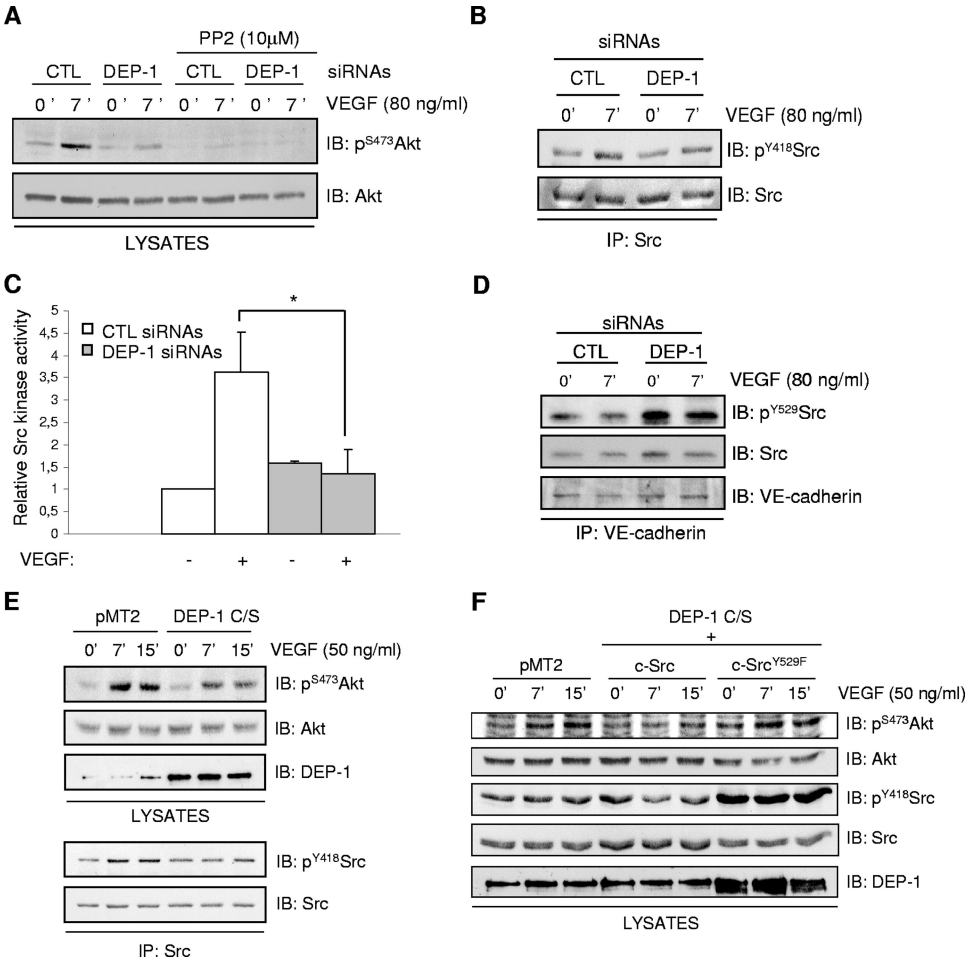

FIG. 6. Src activity is required for VEGF-dependent Akt activation and is impaired in DEP-1-depleted cells. (A) Control (CTL) and DEP-1-depleted HUVECs were preincubated with dimethyl sulfoxide or PP2 (10 μM) for 1 h and then stimulated or not with VEGF (80 ng/ml) for 7 min. Phosphorylation of Akt was determined by immunoblotting (IB) cell lysates (40 μg) with the p^{S473}Akt antibody. (B) Src was immunoprecipitated (IP) from lysates of control and DEP-1-depleted HUVECs stimulated or not with VEGF (80 ng/ml) for the indicated times. Activation of Src was detected by immunoblotting with the phospho-specific antibody recognizing p^{Y418}Src. (C) The kinase activity of Src immunoprecipitated from control and DEP-1-depleted cells, stimulated or not with VEGF (80 ng/ml), was evaluated in an in vitro assay. Results are representative of three independent experiments and are expressed as ratios of activity (± standard deviations) relative to the unstimulated control cells. *, $P < 0.05$. (D) The phosphorylation of Y529 of Src coprecipitating with VE-cadherin was determined in control and DEP-1-depleted cells stimulated or not with VEGF (80 ng/ml). (E) The VEGF-induced activation of Akt (pS473) and Src (pY418) in HUVECs transfected with empty vector (pMT2) or catalytically inactive DEP-1 C/S was determined on total cell lysates and immunoprecipitated Src, respectively. (F) WT or constitutively active Src (Y529F) was cotransfected with DEP-1 C/S in HUVECs. The activation of Akt (pS473) in response to VEGF stimulation (50 ng/ml) was detected on total cell lysates.

Activation of other Src-dependent signaling pathways involved in survival might also be affected in DEP-1-depleted cells and contribute to the promotion of cell death. The activation of Src by DEP-1 was actually reported to increase cell adhesion and FAK tyrosine phosphorylation (36), and the Src-dependent phosphorylation of FAK has been associated with a VEGF-induced survival response (1). In this context, the depletion of DEP-1 in HUVECs could then also lead to weaker cell-substratum adhesion and FAK phosphorylation, and therefore contribute to the defective Akt activation and survival of these cells upon starvation (1, 17, 27). Since Gab1 is a major mediator of the PI3K/Akt pathway that is also phosphorylated by Src kinases in VEGF-stimulated HUVECs (10), our results nevertheless strongly support Gab1 as a key contributor to the activation of this essential survival pathway. Importantly, we have shown for the first time that Gab1 associates with VE-cadherin and β-catenin complexes, which have been shown to associate with VEGFR2 and mediate Akt activation and endothelial cell survival in response to VEGF (8). Moreover, our work reveals that DEP-1 may also modulate activation of this pathway by regulating the ability of Gab1 to associate with these complexes. Thus, the correlation between activation of Akt, cell survival, and the ability of Gab1 to associate with PI3K, Src, β-catenin, VE-cadherin, and VEGFR2 strongly argues in favor of a role for the Gab1 adapter in allowing the recruitment of PI3K to these VE-cadherin/VEGFR2 complexes. The underlying mechanism involved in the formation and regulation of these complexes however remains to be defined. Since the regulation of cell-cell adhesion is mediated via the Src-dependent phosphorylation of proteins such as β-cate-

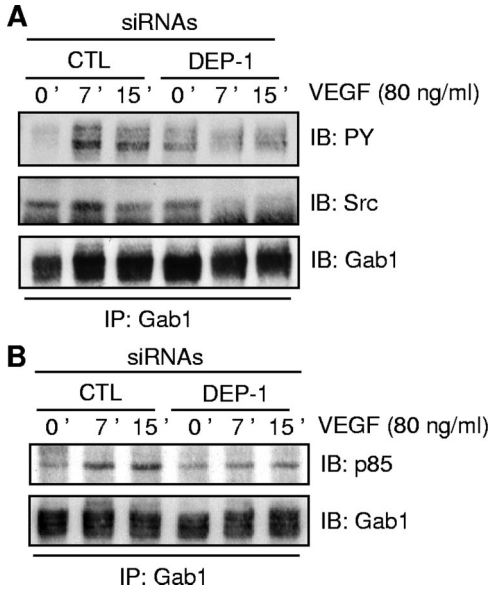

FIG. 7. Depletion of DEP-1 interferes with the Src-sensitive tyrosine phosphorylation of Gab1 and its association with Src and PI3K in response to VEGF stimulation. (A) HUVECs were treated as for Fig. 4. The phosphorylation of immunoprecipitated (IP) Gab1 and its association with Src were assessed by immunoblotting (IB) with the phosphotyrosine PY99 and Src antibodies. The level of immunoprecipitated Gab1 was shown after membrane stripping and reblotting with the Gab1 antibody. (B) The association of immunoprecipitated Gab1 with the p85 subunit of PI3K as well as the level of Gab1 were determined by immunoblotting with the p85 and Gab1 antibodies, respectively.

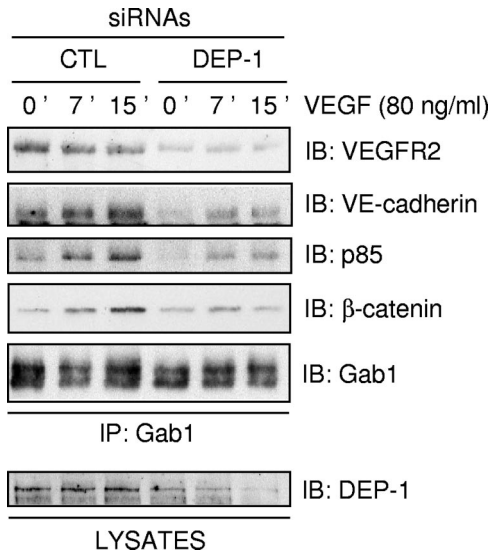

FIG. 8. Gab1 associates with VEGFR2/VE-cadherin complexes, and this is impaired in DEP-1-depleted HUVECs. Control (CTL) and DEP-1-depleted HUVECs were stimulated with VEGF (80 ng/ml) for the indicated times. Gab1 was immunoprecipitated (IP) from the cell lysates, and its association with p85, β-catenin, VE-cadherin, and VEGFR2 was detected by immunoblotting (IB) with the corresponding antibodies. Equal immunoprecipitated Gab1 levels were detected using the Gab1 antibody. The depletion of DEP-1 was confirmed by immunoblotting the cell lysates with the DEP-1 antibody (lower panel).

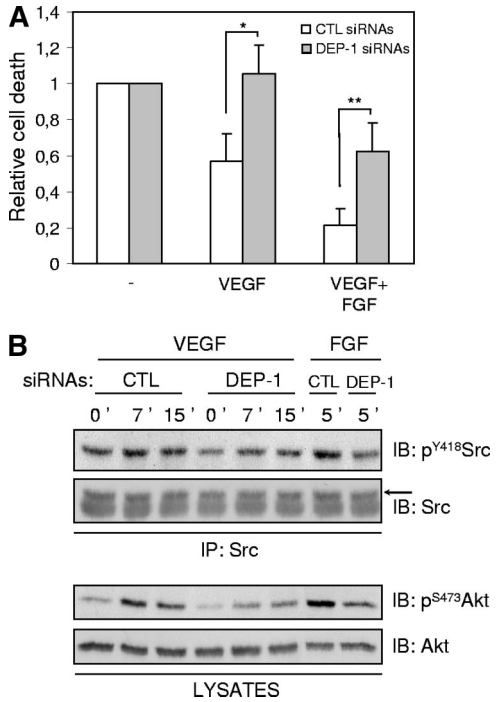

FIG. 9. The depletion of DEP-1 promotes endothelial cell death in response to VEGF and FGF. (A) Control (CTL) and DEP-1-depleted HUVECs were incubated for 33 h in EBM containing 2% FBS alone (-), with VEGF (80 ng/ml), or VEGF (80 ng/ml) with FGF (80 ng/ml) and heparin (5 μg/ml) (VEGF+FGF), as described in Materials and Methods. Collected cells were stained with propidium iodide and prepared for FACS analysis to determine the percentage of dead cells (sub-G1 peak) under the various conditions. Results representative of five independent experiments are expressed as ratios of cell death (± the standard deviation) observed in control or DEP-1-depleted cells grown with survival factors, relative to their corresponding starved cell population. *, $P < 0.0005$; **, $P < 0.005$. (B) DEP-1 is involved in Src and Akt activation in response to FGF. Src was immunoprecipitated (IP) from lysates of control and DEP-1-depleted HUVECs stimulated with VEGF (80 ng/ml) or FGF (50 ng/ml) plus heparin (5 μg/ml) (upper panels). Src activation was determined by immunoblotting (IB) with the p^{Y418}Src antibody. Akt activation was determined by immunoblotting lysates of control and DEP-1-depleted cells with p^{S473}Akt antibodies (lower panels).

nin and $p120^{catenin}$, which are potential DEP-1 substrates, and that DEP-1 associates with β-catenin and colocalizes to these junctions, it is interesting to consider that the depletion of DEP-1 in endothelial cells might also result in their altered phosphorylation and function (6, 25, 44). Future work will be required to determine if such events contribute to the impaired formation of this important signaling complex in DEP-1-depleted cells, which altogether would further amplify the block of Akt activation and survival in response to VEGF.

Interestingly, the phosphorylation of the Akt substrate eNOS on S1177 was found to be increased in DEP-1-depleted cells, even though Akt activation was impaired, as demonstrated by the decreased phosphorylation of both S473 and T308 and the decreased phosphorylation of other Akt substrates, such as FOXO1/4 (19, 37, 38). However, calcium, PKA, and PKC have also been reported to phosphorylate eNOS on S1177 in response to various stimuli (12, 20, 39). Similarly, we have found that a PKC inhibitor, rottlerin, leads to the inhibi-

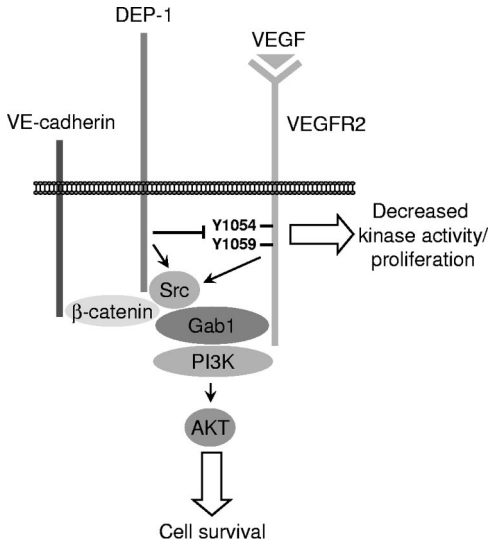

FIG. 10. Model. Expression of DEP-1 at cell-cell adhesions of endothelial cells attenuates VEGFR2 kinase activity and VEGF-mediated endothelial cell proliferation but positively contributes to the recruitment of Gab1 to the VEGFR2/VE-cadherin complex and to the activation of Src and the ensuing phosphorylation of Gab1. This results in the induced association of PI3K to Gab1 and the optimal activation of Akt and endothelial cell survival in response to VEGF.

tion of eNOS phosphorylation without affecting that of Akt (data not shown), demonstrating that this mechanism of eNOS phosphorylation is also active in VEGF-stimulated HUVECs. The role of alternate pathways in allowing the phosphorylation of eNOS may therefore explain how VEGF and hyperactivated VEGFR2 can induce increased phosphorylation of eNOS in DEP-1-depleted cells, in which Akt activation is suboptimal.

This is the first time that a prosurvival function has been attributed to DEP-1, and this may be related to the fact that primary cell cultures instead of immortalized endothelial cells or transformed cancer cells were used for our study. Some of the previous in vitro work was performed on mouse endothelial cells immortalized with the polyomavirus middle T (PymT) oncogene (34). PymT associates with and activates Src kinases and has been reported to constitutively phosphorylate Gab1 and activate Akt (29, 42, 48). Thus, the depletion of DEP-1 in these cells should have no impact on the activation of the Src-Gab1-Akt pathway or cell survival. Moreover, under the experimental conditions for FACS analysis, we have not been able to observe an enhancement of DNA synthesis in DEP-1-depleted cells as previously reported (34). However, this result is consistent with the reduced proliferation of Akt1$^{-/-}$ endothelial cells (9). The in vivo functional inactivation of DEP-1 was reported not to yield any differences in the apoptosis rate of endothelial cells compared to control animals (50). A possible explanation may be that the essential role of Akt in VEGF-mediated survival and angiogenesis is only apparent during postnatal or pathological angiogenesis, but not during developmental angiogenesis (2, 9). Thus, too little expression or activation of DEP-1 during neoangiogenesis could presumably allow increased VEGFR2 phosphorylation and activation of proliferative pathways at a time when cells should become quiescent and establish new cellular contacts, and this would be detrimental to the proper formation and stabilization of new blood vessels. In this context, the increased death of endothelial cells could represent a means of controlling this anarchic proliferation. Conversely, the presence of DEP-1 at cell-cell adhesions of endothelial cells would contribute to the enhanced activation of the Src-Gab1-Akt signaling pathway and to the increased survival of cells as they form new cellular contacts, while downregulating the proliferative signals emanating from VEGFR2. DEP-1 could therefore be involved in the coordinate regulation of Src and VEGFR2 to ensure the proper formation of new capillaries.

DEP-1 is best known for its antiproliferative roles and tumor suppressor functions, suggesting that stimulation of DEP-1 function might represent an interesting therapeutic strategy. Our results however demonstrate that in addition to these functions, DEP-1 is also required for the promotion of optimal VEGF-dependent cell survival. In this context, it is tempting to speculate that inhibition of DEP-1 function during pathological angiogenesis could also represent an alternative therapeutic avenue to explore.

ACKNOWLEDGMENTS

We thank our colleague Estelle Schmidtt for her help with the FACS experiments and Cam Patterson, Martine Roussel, Nicholas Tonks, and Stéphane Laporte for their generous gifts of plasmids. We also thank Nicole Beauchemin, Richard Bertrand, and Michel Tremblay for their helpful comments on the manuscript.

This work was initially supported by the Cancer Research Society Inc. and completed with funds from the Canadian Institutes of Health Research (to I.R.). C.C. was supported by studentships from Université de Montréal (Molecular Biology Programs and the Faculty of Graduate Studies) and the Montreal Cancer Institute (Fondation Marc-Bourgie and Fonds Robert-Bourassa). K.S. was supported by the Montreal Cancer Institute (Fondation Marc-Bourgie).

REFERENCES

1. **Abu-Ghazaleh, R., J. Kabir, H. Jia, M. Lobo, and I. Zachary.** 2001. Src mediates stimulation by vascular endothelial growth factor of the phosphorylation of focal adhesion kinase at tyrosine 861, and migration and anti-apoptosis in endothelial cells. Biochem. J. **360:**255–264.
2. **Ackah, E., J. Yu, S. Zoellner, Y. Iwakiri, C. Skurk, R. Shibata, N. Ouchi, R. M. Easton, G. Galasso, M. J. Birnbaum, K. Walsh, and W. C. Sessa.** 2005. Akt1/protein kinase Bα is critical for ischemic and VEGF-mediated angiogenesis. J. Clin. Investig. **115:**2119–2127.
3. **Benjamin, L.** 2000. The controls of microvascular survival. Cancer Metastasis Rev. **19:**75–81.
4. **Berset, T. A., E. F. Hoier, and A. Hajnal.** 2005. The C. elegans homolog of the mammalian tumor suppressor Dep-1/Scc1 inhibits EGFR signaling to regulate binary cell fate decisions. Genes Dev. **19:**1328–1340.
5. **Blanes, M. G., M. Oubaha, Y. Rautureau, and J.-P. Gratton.** 2007. Phosphorylation of tyrosine 801 of the VEGFR-2 is necessary for AKT-dependent eNOS activation and nitric oxide release from endothelial cells. J. Biol. Chem. **282:**10660–10669.
6. **Borges, L. G., R. A. Seifert, F. J. Grant, C. E. Hart, C. M. Disteche, S. Edelhoff, F. F. Solca, M. A. Lieberman, V. Lindner, E. H. Fischer, S. Lok, and D. F. Bowen-Pope.** 1996. Cloning and characterization of rat density-enhanced phosphatase-1, a protein tyrosine phosphatase expressed by vascular cells. Circ. Res. **79:**570–580.
7. **Carmeliet, P., and R. K. Jain.** 2000. Angiogenesis in cancer and other diseases. Nature **407:**249–257.
8. **Carmeliet, P., M.-G. Lampugnani, L. Moons, F. Breviaro, V. Compernolle, F. Bono, G. Balconi, R. Spagnuolo, B. Oosthuyse, M. Dewerchin, A. Zanetti, A. Angellilo, V. Mattot, D. Nuyens, E. Lutgens, F. Clotman, M. C. de Ruiter, A. Gittenberger-de Groot, R. Poelmann, F. Lupu, J.-M. Herbert, D. Collen, and E. Dejana.** 1999. Targeted deficiency or cytosolic truncation of the VE-cadherin gene in mice impairs VEGF-mediated endothelial survival and angiogenesis. Cell **98:**147–157.
9. **Chen, J., P. R. Somanath, O. Razorenova, W. Chen, N. Hay, P. Bornstein, and T. Byzova.** 2005. Akt1 regulates pathological angiogenesis, vascular maturation and permeability in vivo. Nat. Med. **11:**1188–1196.
10. **Dance, M., A. Montagner, A. Yart, B. Masri, Y. Audigier, B. Perret, J.-P.**

Salles, and P. Raynal. 2006. The adaptor protein Gab1 couples the stimulation of vascular endothelial growth factor receptor-2 to the activation of phosphoinositide 3-kinase. J. Biol. Chem. **281:**23285–23295.
11. **de la Fuente-Garcia, M., J. Nicolas, J. Freed, E. Palou, A. Thomas, R. Vilella, J. Vives, and A. Gaya.** 1998. CD148 is a membrane protein tyrosine phosphatase present in all hematopoietic lineages and is involved in signal transduction on lymphocytes. Blood **91:**2800–2809.
12. **Dixit, M., A. E. Loot, A. Mohamed, B. Fisslthaler, C. M. Boulanger, B. Ceacareanu, A. Hassid, R. Busse, and I. Fleming.** 2005. Gab1, SHP2, and protein kinase A are crucial for the activation of the endothelial NO synthase by fluid shear stress. Circ. Res. **97:**1236–1244.
13. **Eliceiri, B. P., R. Paul, P. L. Schwartzberg, J. D. Hood, J. Leng, and D. A. Cheresh.** 1999. Selective requirement for Src kinases during VEGF-induced angiogenesis and vascular permeability. Mol. Cell **4:**915–924.
14. **Ferrara, N.** 2005. The role of VEGF in the regulation of physiological and pathological angiogenesis, p. 209–231. *In* M. Clauss and G. Breier (ed.), Mechanisms of angiogenesis. Birkhäuser Verlag, Basel, Switzerland.
15. **Ferrara, N., H.-P. Gerber, and J. LeCouter.** 2003. The biology of VEGF and its receptors. Nat. Med. **9:**669–676.
16. **Folkman, J.** 1995. Angiogenesis in cancer, vasculature, rheumatoid and other diseases. Nat. Med. **1:**27–31.
17. **Frisch, S. M., K. Vuori, E. Ruoslahti, and P. Y. Chan-Hui.** 1996. Control of adhesion-dependent cell survival by focal adhesion kinase. J. Cell Biol. **134:** 793–799.
18. **Fujio, Y., and K. Walsh.** 1999. Akt mediates cytoprotection of endothelial cells by vascular endothelial growth factor in an anchorage-dependent manner. J. Biol. Chem. **274:**16349–16354.
19. **Fulton, D., J.-P. Gratton, T. J. McCabe, J. Fontana, Y. Fujio, K. Walsh, T. F. Franke, A. Papapetropoulos, and W. C. Sessa.** 1999. Regulation of endothelium-derived nitric oxide production by the protein kinase Akt. Nature **399:**597–601.
20. **Fulton, D., J.-P. Gratton, and W. C. Sessa.** 2001. Post-translational control of endothelial nitric oxide synthase: why isn't calcium/calmodulin enough? J. Pharmacol. Exp. Ther. **299:**818–824.
21. **Gerber, H. P., A. McMurtrey, J. Kowalski, M. Yan, B. A. Keyt, V. Dixit, and N. Ferrara.** 1998. Vascular endothelial growth factor regulates endothelial cell survival through the phosphatidylinositol 3′-kinase/Akt signal transduction pathway. J. Biol. Chem. **273:**30336–30343.
22. **Guo, D., Q. Jia, H.-Y. Song, R. S. Warren, and D. B. Donner.** 1995. Vascular endothelial cell growth factor promotes tyrosine phosphorylation of mediators of signal transduction that contain SH2 domains. J. Biol. Chem. **270:** 6729–6733.
23. **Ha, C. H., A. M. Bennett, and Z.-G. Jin.** 2008. A novel role of vascular endothelial cadherin in modulating c-Src activation and downstream signaling of vascular endothelial growth factor. J. Biol. Chem. **283:**7261–7270.
24. **He, H., V. J. Venema, X. Gu, R. C. Venema, and M. B. Marrero.** 1999. Vascular endothelial growth factor signals endothelial cell production of nitric oxide and prostacyclin through Flk/KDR activation of c-Src. J. Biol. Chem. **274:**25130–25135.
25. **Holsinger, L. J., K. Ward, B. Duffield, J. Zachwieja, and B. Jallal.** 2002. The transmembrane receptor protein tyrosine phosphatase DEP1 interacts with p120ctn. Oncogene **21:**7067–7076.
26. **Honda, H., J. Inazawa, J. Nishida, Y. Yazaki, and H. Hirai.** 1994. Molecular cloning, characterization, and chromosomal localization of a novel protein-tyrosine phosphatase, HPTP eta. Blood **84:**4186–4194.
27. **Hungerford, J. E., M. T. Compton, M. L. Matter, B. G. Hoffstrom, and C. A. Otey.** 1996. Inhibition of pp125FAK in cultured fibroblasts results in apoptosis. J. Cell Biol. **135:**1383–1390.
28. **Huyer, G., S. Liu, J. Kelly, J. Moffat, P. Payette, B. Kennedy, G. Tsaprailis, M. J. Gresser, and C. Ramachandran.** 1997. Mechanism of inhibition of protein-tyrosine phosphatases by vanadate and pervanadate. J. Biol. Chem. **272:**843–851.
29. **Ichaso, N., and S. M. Dilworth.** 2001. Cell transformation by the middle T-antigen of polyoma virus. Oncogene **20:**7908–7916.
30. **Iervolino, A., R. Iuliano, F. Trapasso, G. Viglietto, R. M. Melillo, F. Carlomagno, M. Santoro, and A. Fusco.** 2006. The receptor-type protein tyrosine phosphatase J antagonizes the biochemical and biological effects of RET-derived oncoproteins. Cancer Res. **66:**6280–6287.
31. **Keane, M., G. Lowrey, S. Ettenberg, M. Dayton, and S. Lipkowitz.** 1996. The protein tyrosine phosphatase DEP-1 is induced during differentiation and inhibits growth of breast cancer cells. Cancer Res. **56:**4236–4243.
32. **Khurana, R., M. Simons, J. F. Martin, and I. C. Zachary.** 2005. Role of angiogenesis in cardiovascular disease: a critical appraisal. Circulation **112:** 1813–1824.
33. **Kovalenko, M., K. Denner, J. Sandström, C. Persson, S. Gross, E. Jandt, R. Vilella, F. Böhmer, and A. Ostman.** 2000. Site-selective dephosphorylation of the platelet-derived growth factor beta-receptor by the receptor-like protein-tyrosine phosphatase DEP-1. J. Biol. Chem. **275:**16219–16226.
34. **Lampugnani, M. G., A. Zanetti, M. Corada, T. Takahashi, G. Balconi, F. Breviario, F. Orsenigo, A. Cattelino, R. Kemler, T. O. Daniel, and E. Dejana.** 2003. Contact inhibition of VEGF-induced proliferation requires vascular endothelial cadherin, β-catenin, and the phosphatase DEP-1/CD148. J. Cell Biol. **161:**793–804.
35. **Laramée, M., C. Chabot, M. Cloutier, R. Stenne, M. Holgado-Madruga, A. J. Wong, and I. Royal.** 2007. The scaffolding adapter Gab1 mediates vascular endothelial growth factor signaling and is required for endothelial cell migration and capillary formation. J. Biol. Chem. **282:**7758–7769.
36. **Le Pera, I., R. Iuliano, T. Florio, C. Susini, F. Trapasso, M. Santoro, L. Chiariotti, G. Schettini, G. Viglietto, and A. Fusco.** 2005. The rat tyrosine phosphatase η increases cell adhesion by activating c-Src through dephosphorylation of its inhibitory phosphotyrosine residue. Oncogene **24:**3187–3195.
37. **Manning, B. D., and L. C. Cantley.** 2007. AKT/PKB signaling: navigating downstream. Cell **129:**1261–1274.
38. **Michell, B. J., J. E. Griffiths, K. I. Mitchelhill, I. Rodriguez-Crespo, T. Tiganis, S. Bozinovski, P. R. O. de Montellano, B. E. Kemp, and R. B. Pearson.** 1999. The Akt kinase signals directly to endothelial nitric oxide synthase. Curr. Biol. **9:**845–848.
39. **Motley, E. D., K. Eguchi, M. M. Patterson, P. D. Palmer, H. Suzuki, and S. Eguchi.** 2007. Mechanism of endothelial nitric oxide synthase phosphorylation and activation by thrombin. Hypertension **49:**577–583.
40. **Munshi, N., J. E. Groopman, P. S. Gill, and R. K. Ganju.** 2000. c-Src mediates mitogenic signals and associates with cytoskeletal proteins upon vascular endothelial growth factor stimulation in Kaposi's sarcoma cells. J. Immunol. **164:**1169–1174.
41. **Olsson, A.-K., A. Dimberg, J. Kreuger, and L. Claesson-Welsh.** 2006. VEGF receptor signalling; in control of vascular function. Nat. Rev. Mol. Cell Biol. **7:**359–371.
42. **Ong, S. H., S. Dilworth, I. Hauck-Schmalenberger, T. Pawson, and F. Kiefer.** 2001. ShcA and Grb2 mediate polyoma middle T antigen-induced endothelial transformation and Gab1 tyrosine phosphorylation. EMBO J. **20:**6327–6336.
43. **Ostman, A., Q. Yang, and N. Tonks.** 1994. Expression of DEP-1, a receptor-like protein-tyrosine-phosphatase, is enhanced with increasing cell density. Proc. Natl. Acad. Sci. USA **91:**9680–9684.
44. **Palka, H. L., M. Park, and N. K. Tonks.** 2003. Hepatocyte growth factor receptor tyrosine kinase Met is a substrate of the receptor protein-tyrosine phosphatase DEP-1. J. Biol. Chem. **278:**5728–5735.
45. **Risau, W.** 1997. Mechanisms of angiogenesis. Nature **386:**671–674.
46. **Royal, I., N. Lamarche-Vane, L. Lamorte, K. Kaibuchi, and M. Park.** 2000. Activation of Cdc42, Rac, PAK and Rho-kinase in response to hepatocyte growth factor differentially regulate epithelial cell colony spreading and dissociation. Mol. Biol. Cell **11:**1709–1725.
47. **Ruivenkamp, C. A. L., T. van Wezel, C. Zanon, A. P. M. Stassen, C. Vlcek, T. Csikos, A. M. Klous, N. Tripodis, A. Perrakis, L. Boerrigter, P. C. Groot, J. Lindeman, W. J. Mooi, G. A. Meijjer, G. Scholten, H. Dauwerse, V. Paces, N. van Zandwijk, G. J. B. van Ommen, and P. Demant.** 2002. Ptprj is a candidate for the mouse colon-cancer susceptibility locus Scc1 and is frequently deleted in human cancers. Nat. Genet. **31:**295–300.
48. **Summers, S. A., L. Lipfert, and M. J. Birnbaum.** 1998. Polyoma middle T antigen activates the Ser/Thr kinase Akt in a PI3-kinase-dependent manner. Biochem. Biophys. Res. Commun. **246:**76–81.
49. **Takahashi, T., K. Takahashi, R. Mernaugh, V. Drozdoff, C. Sipe, H. Schoecklmann, B. Robert, D. R. Abrahamson, and T. O. Daniel.** 1999. Endothelial localization of receptor tyrosine phosphatase, ECRTP/DEP-1, in developing and mature renal vasculature. J. Am. Soc. Nephrol. **10:**2135–2145.
50. **Takahashi, T., K. Takahashi, P. L. St. John, P. A. Fleming, T. Tomemori, T. Watanabe, D. R. Abrahamson, C. J. Drake, T. Shirasawa, and T. O. Daniel.** 2003. A mutant receptor tyrosine phosphatase, CD148, causes defects in vascular development. Mol. Cell. Biol. **23:**1817–1831.
51. **Trapasso, F., R. Iuliano, A. Boccia, A. Stella, R. Visconti, P. Bruni, G. Baldassarre, M. Santoro, G. Viglietto, and A. Fusco.** 2000. Rat protein tyrosine phosphatase η suppresses the neoplastic phenotype of retrovirally transformed thyroid cells through the stabilization of $p27^{Kip1}$. Mol. Cell. Biol. **20:**9236–9246.
52. **Tsujikawa, K., T. Ichijo, K. Moriyama, N. Tadotsu, K. Sakamoto, N. Sakane, S.-i. Fukada, T. Furukawa, H. Saito, and H. Yamamoto.** 2002. Regulation of Lck and Fyn tyrosine kinase activities by transmembrane protein tyrosine phosphatase leukocyte common antigen-related molecule. Mol. Cancer Res. **1:**155–163.
53. **Xia, P., L. P. Aiello, H. Ishii, Z. Y. Jiang, D. J. Park, G. S. Robinson, H. Takagi, W. P. Newsome, M. R. Jirousek, and G. L. King.** 1996. Characterization of vascular endothelial growth factor's effect on the activation of protein kinase C, its isoform, and endothelial cell growth. J. Clin. Investig. **9:**2018–2026.
54. **Zhang, L., M. Martelli, C. Battaglia, F. Trapasso, D. Tramontano, G. Viglietto, A. Porcellini, M. Santoro, and A. Fusco.** 1997. Thyroid cell transformation inhibits the expression of a novel rat protein tyrosine phosphatase. Exp. Cell Res. **235:**62–70.
55. **Zhu, J. W., T. Brdicka, T. R. Katsumoto, J. Lin, and A. Weiss.** 2008. Structurally distinct phosphatases CD45 and CD148 both regulate B cell and macrophage immunoreceptor signaling. Immunity **28:**183–196.